

## Physico-chemical and electrochemical properties of nanoparticulate NiO/C composites for high performance lithium and sodium ion battery anodes

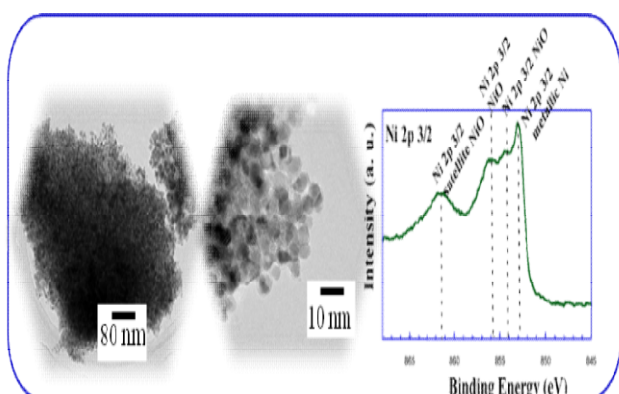
Amaia Iturrondobeitia (amaia.iturrondobeitia@ehu.eus)<sup>a</sup>, Aintzane Goñi (aintzane.goni@ehu.eus)<sup>a,b</sup>, Izaskun Gil de Muro (izaskun.gildemuro@ehu.eus)<sup>a,b</sup>, Luis Lezama (luis.lezama@ehu.eus)<sup>a,b\*</sup>, Teófilo Rojo (trojo@cicenergigune.es)<sup>a,c</sup>,

<sup>a</sup> Departamento de Química Inorgánica, Universidad del País Vasco UPV/EHU, P.O. Box 644, 48080, Bilbao, Spain.

<sup>b</sup> BCMATERIALS, Ibaizabal Bidea 500, Parque Científico y Tecnológico de Bizkaia, 48160, Derio, Spain

<sup>c</sup> CIC energiGUNE, Parque Tecnológico de Álava. Albert Einstein 48, 01510 Miñano, Álava, Spain.

### Graphical Abstract



### Abstract.

Nanoparticulate NiO and NiO/C composites with different carbon proportions have been prepared for anode application in lithium and sodium ion batteries. Structural characterization demonstrated the presence of metallic Ni in the composites. Morphological study revealed that the NiO and Ni nanoparticles were well dispersed in the matrix of amorphous carbon. The electrochemical study showed that the lithium ion batteries (LIBs) containing composites with carbon have promising electrochemical performances delivering specific discharge capacities of 550 mAh/g after operating for 100 cycles at 1C. These excellent results could be explained by the homogeneity of particle size and structure as well as the uniform distribution of NiO/Ni nanoparticles in the *in situ* generated amorphous carbon matrix. On the other hand, the sodium ion battery (NIB) with the NiO/C composite revealed a poor cycling stability. Post-mortem analyses revealed that this fact could be ascribed to the absence of a stable SEI or passivation layer upon cycling.

## Introduction

.As one of the most important and widely used rechargeable power sources, lithium ion batteries (LIBs) have been widely used in portable electronics, electric vehicles (EVs) and hybrid electric vehicles(HEVs)<sup>14</sup>.

Additionally, they are supposed to be one of the most promising candidates for next generation power sources. Besides of LIBs, recently, sodium ion batteries (NIBs) have received increased attention as an alternative to LIBs for stationary storage due to the abundance and low cost of Na. Actually, NIBs were initially studied when the development of LIBs began in the 1970s, but due to the fast advances in the development of LIBs, NIBs were unregarded<sup>5</sup>. Even if the fundamental principles of the NIBs and LIBs are almost the same, NIBs usually exhibit low specific capacities, short cycle lifes and poor rate capabilities due to increased radius and mass of Na (1.02Å, 22.99 g/mol) compared to that of Li (0.59Å, 6.94 g/mol)<sup>6</sup>. Additionally, sodium has a higher standard electrode potential compared to lithium (-2.71 V vs SHE as compared to -3.02 V vs SHE for lithium). Consequently, NIBs will often fall short in terms of energy<sup>7</sup>. Nevertheless, the weight of cyclable lithium and sodium is only a small part of the mass of the components of the electrode.

Nowadays, even if graphite is the most widely used anode material due to its low cost, high abundance, and outstanding electrochemical performance, this material exhibits a theoretical capacity of 372 mAh/g. Consequently, in order to fulfill the requirements as to large scale applications, higher energy density systems need to be developed. This purpose implies the necessity of denser and higher capacity anode materials are needed.

In this sense, 3d transition metal oxides (MO<sub>x</sub>) are among one of the most promising next-generation anode materials under consideration due to their low cost, high theoretical capacities (500-1000 mAh/g) and easy fabrication<sup>8,9</sup>.

NiO has been regarded as one of the most popular choices of metal oxides due to its high theoretical capacity (718 mAh/g), high corrosion resistance and low materials and processing costs<sup>10</sup>. However, further optimization of nickel oxides as anode materials is needed due to their poor capacity retention or rate capability owed to low electric conductivity and large volume change during the conversion reaction<sup>11,12</sup>.

Even if transition metal oxides have been extensively studied in LIBs, only a few metal oxides have been studied for application in NIBs<sup>13, 14</sup>. Among these studies, some previous reports have demonstrated the potential application of NiO in NIBs<sup>15</sup>. Meanwhile, other researchers have revealed the electrochemical inactivity of NiO with Na, while exhibiting outstanding performances in LIBs. In this regard, the reason why this is happening is not clearly understood yet<sup>16</sup>. As far as we are aware, very little research has been done in the field of NiO anodes for NIBs application up to now.

In this study, three different composites based on nanosized NiO and carbon, were successfully synthesized by the freeze-drying method. We report on the structural, morphologic, magnetic, spectroscopic and electrochemical characterization (vs Li and Na) of the synthesized samples, establishing correlations among the composition, morphology and electrochemical performance. Particular attention has been paid to the post-mortem analysis of NIBs in order to understand why the same material behaves differently when applied as anode for LIBs and NIBs.

## Materials and Methods

Three nickel oxide samples were synthesized by the freeze-drying method. For the sample designated NiO<sub>air</sub> only Ni(NO<sub>3</sub>)<sub>2</sub>·6 H<sub>2</sub>O was dissolved in 25 ml of water. For the other two samples

$C_6H_8O_7 \cdot H_2O$  and  $Ni(NO_3)_2 \cdot 6 H_2O$  reagents were added in the molar ratios of 0.25:1 and 1:1, in order to produce composites with different carbon contents. The resulting solutions were subsequently frozen in a round-bottom flask that contained liquid nitrogen. Afterwards, the round bottom flasks were connected to the freeze-dryer for 48 h at a pressure of  $3 \cdot 10^{-1}$  mbar and a temperature of  $-80^\circ C$  to sublime the solvent. The as-obtained precursors were subjected to a single heat treatment at  $400^\circ C$  for 6h. The heat treatment of the NiO<sub>air</sub> sample was carried out in air while the other two samples were calcined in a nitrogen atmosphere. Subsequently, the products were ball-milled for 30 minutes.

A Perkin-Elmer 2400CHN analyzer was employed to determine the carbon content of the samples. Structural characterization of the samples was carried out using X-ray powder diffraction with a Bruker D8 Advance Vario diffractometer using  $CuK\alpha$  radiation. The obtained diffractograms were profile-fitted using the FullProf program<sup>17</sup>. The morphologies of the materials were studied by Transmission Electron Microscopy (TEM) using a FEI TECNAI F30 and by a scanning electron microscope (JEOL JSM 7500F) and by Scanning Electron Microscopy (SEM) (JEOL JSM 7500F). Magnetic susceptibility measurements (dc) were carried out at 300K with a Quantum Design SQUID magnetometer. X-ray photoelectron spectra (XPS) were obtained on a SPECS system equipped with a Phoibos 150 1D-DLD analyzer and a monochromatic  $AlK_{\alpha}$  (1486.6 eV) source. Raman spectroscopy was carried out using a InVia Raman spectrometer using  $Ar^+$  laser excitation with a wavelength of 514 nm.

2032 coin cells were assembled to evaluate the electrochemical performances of the samples. To prepare the electrodes, the active materials were mixed with conducting carbon black (Super P, Timcal) and polyvinylidene fluoride (PVDF) binder with weight ratios of 70:15:15 and dispersed in N-methyl-2-pyrrolidone (NMP) to form a slurry. The slurry was then cast onto Cu current collectors and dried at  $120^\circ C$  in a vacuum oven overnight. For the lithium ion batteries, electrochemical cells with metallic lithium foils as counter electrodes, Celgard 2400 polypropylene separators and 1 M  $LiPF_6$  in 50%-50% ethyl carbonate (EC) and dimethyl carbonate (DMC) as the electrolytic solution, were assembled in an Ar-filled glove box. For the sodium ion batteries, metallic sodium foils were used as counter electrodes. The electrolyte was 1 M  $NaPF_6$  in 50%-50% ethyl carbonate (EC) and dimethyl carbonate (DMC) solution with 1 wt % FEC. All the electrochemical and electrochemical measurements were carried out on a Bio-Logic VMP3 potentiostat/galvanostat at room temperature. Typical electrode loadings were 1.3 mg/cm<sup>2</sup>.

## Results and Discussion

Elemental analysis revealed that the samples contained an average amount of carbon of 0, 18 and 29%. Accordingly, the samples were called NiO<sub>18%C</sub>, NiO<sub>29%C</sub> and NiO<sub>air</sub> as this material was calcined in air.

The structural characterization by XRD showed that for the NiO<sub>air</sub> sample, all of the diffraction peaks could be indexed to pure phase cubic nickel oxide. No additional reflections were detected indicating the absence of impurities. In the case of NiO<sub>18%C</sub> two weak reflections can be detected at  $2\theta \approx 45^\circ$  and  $53^\circ$  corresponding to metallic nickel (Powder Diffraction File 88-2326 PDF card). However, different from NiO<sub>air</sub> and NiO<sub>18%C</sub> samples, the diffraction maxima of NiO<sub>29%C</sub> composite appears to have less intensity and higher broadening. Additionally, the reflections corresponding to metallic nickel have higher intensity in this sample than in the former ones. This could be attributed to the higher amount of carbon in this sample, as it probably has led to a more reducing atmosphere and consequently, a higher amount of Ni (II) has been reduced to Ni(0).

SEM images allowed asserting that the NiO\_air sample is composed of irregularly shaped particles with a wide range of size (5-50 nm). In the same way, NiO\_18%C and NiO\_29%C composites seemed to contain nanoparticles homogeneously dispersed in the in situ generated carbon matrix. In order to further investigate that morphology, TEM measurements were carried out. **Figures 1a, 1b** and **1c** show transmission electron micrographs of the NiO\_air, NiO\_18%C and NiO\_29%C samples. It can be deduced that the NiO\_29%C composite is made up of 5-10 nm homogeneous spherical nanoparticles embedded in the in situ generated carbon matrix. The particle size of NiO\_29%C sample was the smallest of all the samples as the high amount of carbon in this composite acted preventing the growth of particle size.

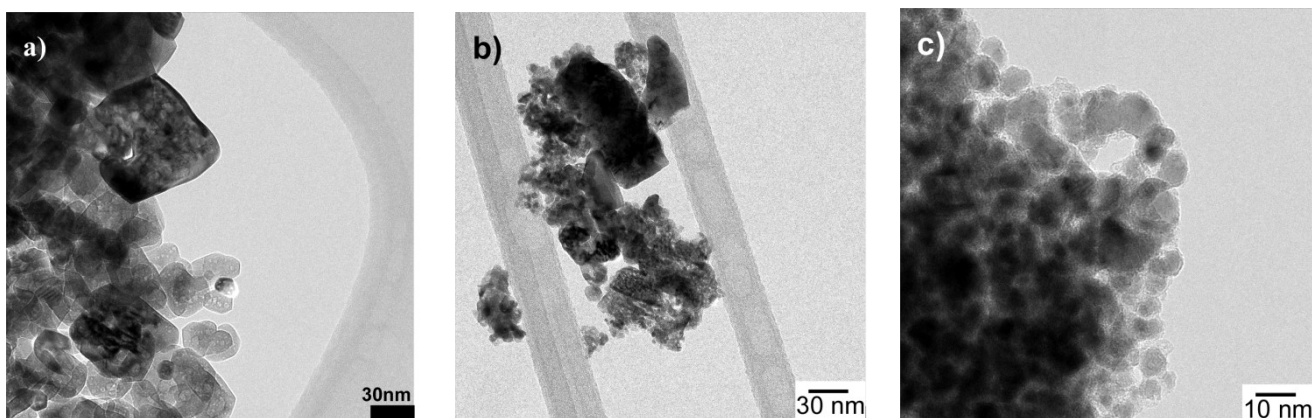


**Figure 1.** TEM images of a) NiO\_air, b) NiO\_18%C and c) NiO\_29%C samples.

The magnetic hysteresis loops at room temperature of the NiO\_air, NiO\_18%C and NiO\_29%C samples exhibited that the samples contain <1, 5 and 41% of metallic nickel, respectively. On the other hand, Raman spectroscopy measurements showed that NiO\_18%C and NiO\_29%C samples have a typical Raman spectrum of non-graphitic carbons. Both of them show two pronounced peaks, one located at  $\approx 1600\text{ cm}^{-1}$  which corresponds to the G-band and is ascribed to the  $E_{2g}$  graphitic mode. The other band located at  $\approx 1340\text{ cm}^{-1}$ , D-band, corresponds to a defect induced mode<sup>18</sup>. Thus, the presence of the D band indicates that the in situ generated carbon is a typically non-graphitizable carbon.

To evaluate the electrochemical performance, lithium half-cells containing NiO\_air and NiO\_18%C and NiO\_29%C composite materials were discharged at current densities corresponding to C/10 and 1C rates.

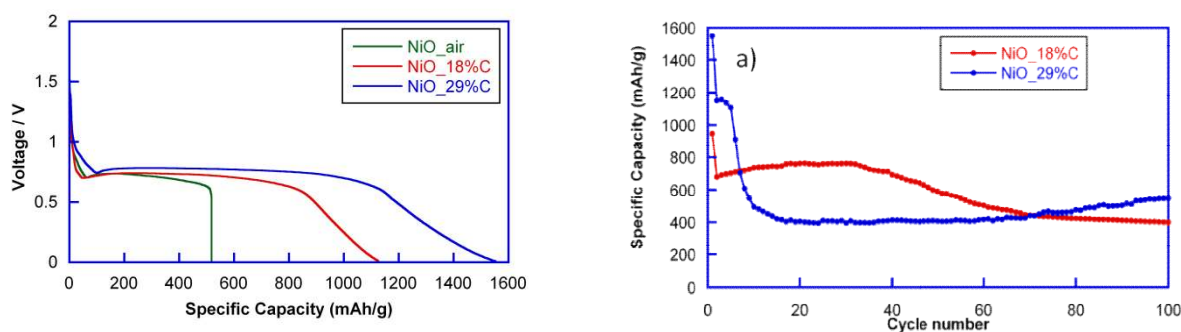


**Figure 2.** First discharge curves for NiO\_air, NiO\_18%C and NiO\_29%C at C/10 and cyclability of the samples

As it can be seen, NiO\_29%C composite is the one that shows the best electrochemical performance as it has a smaller particle size, a more homogeneous appearance and higher carbon and metallic nickel

contents. Due to the synergistic effect that these factors could produce, the electrochemical behavior of NiO\_29%C is better in all aspects.

NiO\_29%C composite was selected to test it versus metallic sodium due to its good lithium storage behavior. **Figure 3** shows the first two discharge-charge curves of NiO\_29%C versus metallic sodium at C/10. As it can be observed, the capacity drastically decays from the third cycle on.

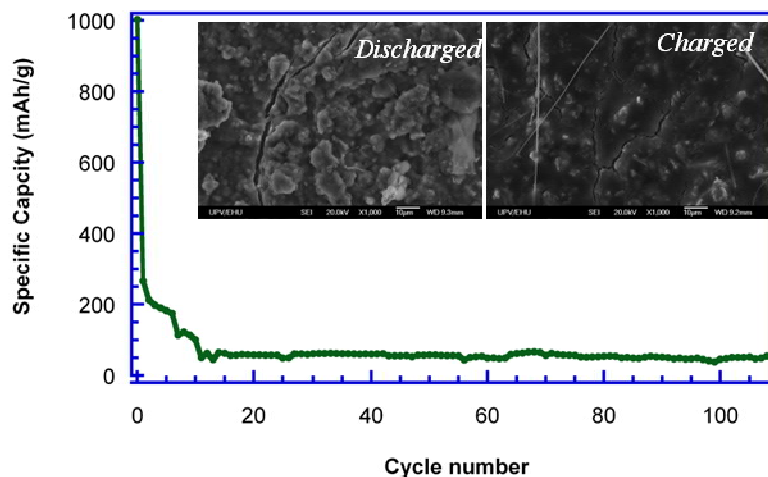


**Figure 3.** Cyclability of NiO\_29%C sample and SEM micrographs of the discharged and charged electrode.

In order to investigate the origin of the capacity fade, a post-mortem study of the sodium half cells containing NiO\_29%C was performed. Post-mortem analyses (ex.situ XRD, SEM, magnetic measurements, XPS and FTIR) revealed that the capacity decay could be mainly ascribed to the absence of a stable SEI upon cycling.

### Conclusions

. NiO\_air, NiO\_18%C and NiO\_29%C samples were successfully prepared by a freeze-drying method. X ray diffraction measurements for NiO\_air sample showed that all of the diffraction peaks could be indexed to nickel oxide. For NiO\_18%C and NiO\_29%C, metallic nickel was detected as well as nickel oxide. The morphologic study demonstrated the heterogeneity of NiO\_air sample with an average particle size of 5-50 nm. However, NiO\_18%C and NiO\_29%C are more homogeneous, have smaller particle size and present an in situ generated amorphous carbon matrix. The most significant result was the reduction of particle size with the increasing of carbon amount. Magnetic measurements allowed calculating the amount of metallic nickel for each sample. NiO\_air, NiO\_18%C and NiO\_29%C samples were employed in LIBs and NiO\_29%C composite was the one with the highest specific capacity, best cycleability, highest coulombic efficiency and best rate discharge capability. This fact could be ascribed to the higher amount of metallic nickel and carbon, the smaller particle size and the homogeneous character that this sample has in comparison to the other materials. On the other hand, the NIB with the NiO\_29%C composite revealed a poor cycling stability. Post-mortem analyses (ex.situ XRD, SEM, magnetic measurements, XPS and FTIR) revealed that this fact could be mainly ascribed to the absence of a stable SEI upon cycling. In this regards, the surface reaction that occurs when discharging (reduced carbon) and charging (NaCO<sub>3</sub>R) the electrode, implies a huge volume expansion causing the fracture of the electrode and leading therefore, to a poor electrochemical performance of the NIB. Additionally, the large amount of carbon that NiO\_29%C

composite contains is another important factor to be considered since the storage of Na into carbon is very limited. Consequently, the diffusion pathways could be blocked promoting the deterioration of the kinetics of the conversion reaction.

## References

- <sup>1</sup> B. Scrosati., Challenge of portable power, *Nature*, 373 (1995) 557.
- <sup>2</sup> J. M. Tarascon, M. Armand., Issues and challenges facing rechargeable lithium batteries, *Nature*, 414 (2001) 359.
- <sup>3</sup> T. Nagaura, K. Tozawa., Lithium ion rechargeable battery, *Prog. Batteries Sol. Cells*, 9 (1990) 209.
- <sup>4</sup> Y. Nishi., The development of lithium ion secondary batteries, *Chem. Rec.*, 1 (2001) 406.
- <sup>5</sup> P. A. Adelhelm, P. Hartmann, C. L. Bendar, M. Busche, C. Enfinger, J. Janek, From lithium to sodium: cell chemistry of room temperature sodium-air and sodium-sulfur batteries, *Beilstein JNanotechnol.*, 6 (2015) 1016.
- <sup>6</sup> Y. Liu, N. Zhang, C. Yu, L. Jiao, J. Chen, MnFe<sub>2</sub>O<sub>4</sub>@C Nanofibers as High-Performance Anode for Sodium-Ion Batteries, *Nano Lett.*, 16 (2012) 3321.
- <sup>7</sup> J.Y. Hwang, S.T. Myung, Y.K. Sun, Sodium-ion batteries: present and future, *Chem. Soc. Rev.*, DOI: 10.1039/c6cs00776g
- <sup>8</sup> P. G. Bruce, B. Scrosati, J. M. Tarascon., Nanomaterials for rechargeable lithium batteries, *Angew. Chem. Int. Ed.*, 47 (2008) 2930-2946.
- <sup>9</sup> P. Poizot, S. Laruelle, S. Grugeon, L. Dupont, J. M. Tarascon., Nano-sized transition-metal oxides as negative-electrode materials for lithium-ion batteries, *Nature*, 407 (2000) 496-499.
- <sup>10</sup> J. Chen, L. N. Xu, W. Y. Li, X. L. Gou.,  $\alpha$ -Fe<sub>2</sub>O<sub>3</sub> nanotubes in gas sensor and lithium-ion battery applications, *Adv. Mater*, 17 (2005) 582-586.
- <sup>11</sup> Y. Zou, Y. Wang., NiO nanosheets grown on graphene nanosheets as superior anode materials for Li-ion batteries, *Nanoscale*, 3 (2011) 2615-2620.
- <sup>12</sup> L. Liu, H. Guo, J. Liu, F. Qian, C. Zhang, T. Li, W. Chen, X. Yang, Y. Guo, Self-assembled hierarchical yolk-shell structured NiO@C from metal-organic frameworks with outstanding performance for lithium storage, *Chem. Commun.*, 50 (2014) 9485-9488.
- <sup>13</sup> S. Hariharan, K. Saravanan, V. Ramar, P. Balaya, A rationally designed dual role anode material for lithium-ion and sodium-ion batteries: case study of eco-friendly Fe<sub>3</sub>O<sub>4</sub>, *Phys. Chem. Chem. Phys.*, 15 (2013) 2945.
- <sup>14</sup> Z. G. Wu, Y. J. Zhong, J. Liu, J. H. Wu, X. D. Guo, B. H. Zhong, Z. Y. Zhang, Subunits controlled synthesis of  $\alpha$ -Fe<sub>2</sub>O<sub>3</sub> multi-shelled core-shell microspheres and their effects on lithium/sodium ion battery performances, *J. Mater. Chem.*, 3 (2015) 10092.
- <sup>15</sup> Y. Jiang, M. Hu, D. Zhang, T. Yuan, W. Sun, B. Xu, M. Yan, Transition metal oxides for high performance sodium ion battery anodes, *Nano Energy*, 5 (2014) 60.
- <sup>16</sup> Q. Sun, Q.Q. Ren, H. Li, Z.W. Fu, High capacity Sb<sub>2</sub>O<sub>4</sub> thin film electrodes for rechargeable sodium battery, *Electrochem. Commun.*, 13 (2011) 1462.
- <sup>17</sup> Rodríguez-Carvajal J., <http://valmap.dfis.ull.es/fullprof/index.php>.
- <sup>18</sup> C. Kim, K. S. Yang, M. Kojima, K. Yoshida, Y. J. Kim, Y. A. Kim, M. Endo, Fabrication of Electrospinnig-derived carbon nanofiber webs for the anode material of Lithium-Ion Secondary Battery, *Adv. Funct. Mater*, 16 (2006) 2393.